

Andisol and microcrystalline cellulose from *Typha angustifolia* for auramine O adsorption

Pranoto Pranoto, Venty Suryanti, Robi'atul Adawiyah

Program Study of Chemistry, Faculty of Mathematics and Natural Sciences, Sebelas Maret University, Surakarta, Indonesia

Article Info

Article history:

Received Sep 7, 2022

Revised Oct 14, 2022

Accepted Nov 21, 2022

Keywords:

Adsorption

Andisol

Hydrolysis

Langmuir

Microcrystalline cellulose

ABSTRACT

Andisol has a large surface area, is mesoporous, and contains the active groups' silanol (Si-OH) and aluminol (Al-OH). Besides andisol, cellulose is a good adsorbent, because microcrystalline cellulose has an active hydroxyl group (OH). The number of active adsorbent groups can be enhanced by chemically modifying the surface area (increment), or adding other materials. These modifications included alkaline modified-andisol with the addition of NaOH to increase pore size, cellulose hydrolysis with HCl to increase surface area, and andisol modification with the inclusion of other materials, mainly cellulose, to increase surface area. After the adsorption process is complete, the adsorption capacity of andisol-microcrystalline cellulose (AMS) to auramine O (AO) is known. As an adsorbent for AO, the surface area of BET andisol is 25.92 m²/g and the pore diameter is 14.40 nm, while the surface area of microcrystalline cellulose and AMS adsorbent are 26.60 m²/g and 18.60 m²/g, respectively. The maximum AO adsorption conditions by AMS were at pH 7, optimum at a contact time of 5 minutes, and maximum at a concentration of 40 mg/L with an adsorbent ratio of 1:1. The adsorption kinetics and isotherm more closely followed the pseudo second-order and Langmuir isotherm with an adsorption capacity of 5.24 mg/g.

This is an open access article under the [CC BY-SA](#) license.



Corresponding Author:

Pranoto Pranoto

Program Study of Chemistry, Faculty of Mathematics and Natural Sciences, Sebelas Maret University

Ir. Sutami Street 36 A, Kentingan, Surakarta 67126, Indonesia

Email: pakpranotomipa@staff.uns.ac.id

1. INTRODUCTION

The textile industry is a major contributor to dye waste. A total of 700,000 tonnes of dye are produced each year, with roughly 100,000 tonnes accessible for commercial use. This extensive use and production on a huge scale have the potential to pollute the environment and cause serious health issues [1]. Annually, over 200 billion liters of waste are generated and disposed of directly into the environment. Dye disposal in water raises chemical oxygen demand (COD) and leads to eutrophication of the water surface [1], [2]. The hydrochloride salt of auramine O (AO) (4, 4'-dimethylaminobenzophenonimide) [3] is a commonly used dye for dyeing paper, leather, silk, linen, cotton, textiles, and bamboo. AO can induce cancer and has a negative impact on kidney and liver function [4]. Therefore, a method for treating waste such as AO dye is needed.

The adsorption method is one of the waste treatment processes with a simple, low-cost, effective, efficient, and reusable process for the next waste treatment cycle [5]. A good adsorbent is selected from a material that is insoluble in water, and has good mechanical stability, chemical stability, and thermal stability. Active groups on the surface of the adsorbent are also needed to interact with pollutants [1].

Andisol can be used as an adsorbent because it has a mesoporous size [6], can be found easily, is relatively inexpensive [7], has an active group, and has a high cation exchange capacity [7]. Andisol is a clay

with a large surface area that contains silanol (Si-OH) and aluminol (Al-OH) active groups. Andisol's active group interacts with positively charged metal ions [8]. Aside from andisol, cellulose is a natural adsorbent that is widely available, tough fiber, biodegradable, biocompatible, protective of plant cell walls, and insoluble in water. Cellulose has three hydroxyl groups in its glucopyranose unit, which gives it the above-mentioned properties. This hydroxyl group is useful for ion exchange, so cellulose can be used as an adsorbent [9], [10]. The hydroxyl active group of the negatively charged CH_2OH compound becomes CH_2O^- and then binds to the positive charge of the dye or metal ion [11].

The adsorption performance can be improved in several ways including increasing the pore size [6], increasing the surface area and adding active groups [8]. The pore size of activated andisol can be up to 5.46 nm [12], which can be increased by treating andisol in acidic (pH 4) or basic (pH 10) pH as activation using HCl or NaOH [6]. Cellulose is not a porous material, so to increase its adsorption performance, increase the number of active groups. The active group will increase as the surface area increases. The surface area of activated andisol can have a size of up to 142.40 m^2/g [12], while the surface area of microcrystalline cellulose is 1.32 m^2/g and the pore size including mesopores is 22.72 nm. The surface area is increased by reducing the particle size of the adsorbent or modifying it. Enzymatic hydrolysis using acid is easier to remove the amorphous phase of cellulose. This results in shorter and more numerous crystals, thereby reducing the degree of polymerization [13]. Another factor that can improve the adsorption performance is by modifying the adsorbent. Adsorbent modification can be done by chemical modification or adding other materials. Modifying the adsorbent can increase the pore size and increase the adsorption capacity [14].

Andisol modified with other materials had a higher adsorption capacity than without modification. An example is the modification of andisol with several other materials such as sugar palm fiber as an adsorbent for Fe (III) [15], Bekonang soil for adsorption of Cu (II) metal [16], and *Agrobacterium sp.* for the bioremediation of Fe (III) metal [9]. Cellulose modified with clay also has an adsorption efficiency of more than 90% [11]. For example, in nanocellulose modified with montmorillonite for methylene blue adsorption [17], modified cellulose with kaolinite for adsorption of congo red [18], and cellulose and clay as bioanocomposites to absorb Drimarine yellow HF-3GL [19].

Therefore, this study will discuss the surface area and pore diameter of andisols, the surface area of microcrystalline cellulose from *Typha angustifolia*, and andisol-microcrystalline cellulose (AMS) adsorbent for the adsorption of AO dye. pH, contact time, solution concentration, and AMS adsorbent ratio. Finally, to determine the adsorption capacity of AO by AMS adsorbent.

2. RESEARCH METHOD

2.1. Isolation of microcellulose

Microcellulose was made by cutting the narrow leaf cattail plant (*Typha angustifolia L.*) into cubes, then dried in the sun to dry and turn brown in color. Lembang plants were blended to become powder and sieved to a size of 20 mesh.

Typha angustifolia L. powder was taken as much as 30 grams and then added with 4% NaOCl up to two times for 4 hours at 80 °C with stirring, where after each addition of NaOCl, it was neutralized first with distilled water to pH 7. The next step was stirring with the addition of NaOH 17.5% for 3 hours at 45 °C, then neutralizing with distilled water. Furthermore, the hydrolysis process was done by adding 4 M HCl for 3 hours at a temperature of 65 °C under hydrothermal conditions. Neutralization was carried out again to pH 7. Furthermore, the cellulose was sonicated for up to 10 minutes, then dried in an oven at 50 °C.

2.2. Andisol activation

Andisol soil was cleaned by washing it with water, then drying it in the open air. Andisol was ground until smooth, then sieved to 150 mesh. The treatment was continued with immersion into distilled water and filtered again. Then dried at 105 °C for 4 hours. Then it was mixed with 250 ml of 3 M NaOH at 70 °C for up to 5 hours. Andisol soil was washed with distilled water until neutral and then calcined for 3 hours at a temperature of 400 °C.

2.3. Modification of AMS

Adsorbent ratios were made in several comparisons namely AMS1 (1:0), AMS2 (2:1), AMS3 (1:1), AMS4 (1:2), AMS5 (0:1). AMS 1:1 is made from andisol as much as 100 mg was dispersed in 2 ml of acetone with constant stirring (200 rpm) for 30 minutes until smooth. Then 100 mg microcellulose in 2 ml acetone was added slowly with constant stirring. The mixture was stirred for up to 12 hours under stirring, then dried. The resulting suspension was rinsed with distilled water and dried in an oven at 40-45 °C to dryness, finally left at room temperature. AMS, andisol, and microcellulose materials were characterized

using Fourier transform infrared (FTIR) Shimadzu Type IRprestige21, x-ray diffraction (XRD) Bruker D2 Phaser, scanning electron microscope (SEM) JEOL JSM-6510LA, surface area analyzer (SAA) Quantachrome instruments type nova 1200e.

2.4. Test method

Microcellulose was isolated from narrow leaf cattail plant (*Typha angustifolia L.*), then modified with andisol soil to adsorb AO. Several variations were carried out under certain conditions, including pH variations carried out at pH 5, 6, 7, and 8 and contact times 5, 10, 30, 50, 70, 90, and 120 minutes. The adsorption isotherm requires variations in concentration, which are at concentrations of 20, 40, 60, 80, and 100 mg/L. The concentration of remaining AO was determined using UV-Visible Spectrophotometry (UV-1900 Series).

3. RESULTS AND DISCUSSION

3.1. AMS materials characterization

Figure 1 shows Fourier transform infrared (FTIR), and Figure 1(a) is a presentation of FTIR data from andisol. The Si-OH/Al-OH bond is shown at a wavelength of 3500.95 cm^{-1} , 1668.42 cm^{-1} for the H-OH bond, a peak of about 1010.74 cm^{-1} is Si-O-Si, and for a peak of about $572\text{-}439\text{ cm}^{-1}$ is for Si-O/Al-O bonds. While the peak of 2315 , 1668 , and 715 cm^{-1} in activated andisol is an impurity that enters the andisol [16].

Peaks of 1609 and 2907 cm^{-1} indicate O-H and C-H stretch, respectively [20], [21]. The peak in the $3400\text{-}3300\text{ cm}^{-1}$ region is the O-H bond of water. The peaks around 1368 , $1160\text{-}1050$, and 899 cm^{-1} are absorption peaks from stretching CH and CO (polysaccharide ring), COC and CO (pyranose ring) and CH oscillation of β -glycosidic bonds [20], [3], [22] The above-mentioned peaks are present in all spectrums of cellulose that have gone through the process of alkalization and hydrolysis as shown in Figure 1(b).

AMS FTIR analysis data are shown in Figure 1(c). The peaks of AMS are similar to those of andisol and microcellulose. The peak at about 3350.50 cm^{-1} is the hydroxyl group of microcellulose. In the AMS spectra, there were peaks at 2910.71 cm^{-1} ; 1058.97 cm^{-1} ; 558.42 cm^{-1} ; and 468.72 cm^{-1} showing stretching of C-H bonds, overlapping Si-O and C-O bonds, and vibration bending of Si-O-Si bonds and bending of Al-O-Al [15].

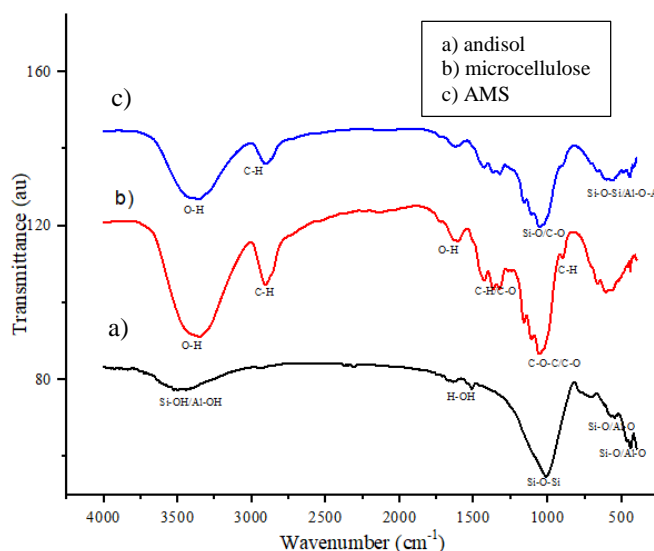


Figure 1. FTIR of (a) andisol, (b) microcellulose, and (c) AMS

Figure 2 shows an XRD graph of AMS, microcrystalline cellulose, and andisol, based on Figure 2(a) shows the diffractogram of the AMS has similar peaks between microcellulose (Figure 2(b)) and andisol (Figure 2(c)). The peaks similar to microcellulose in the AMS were (2θ) 21.98° (crystalline cellulose I) [22], while the peaks similar to andisol in the AMS were (2θ) 27.81° (allophane); and 30.29° ; 35.52° ; 51.55° (kaolinite) [15].

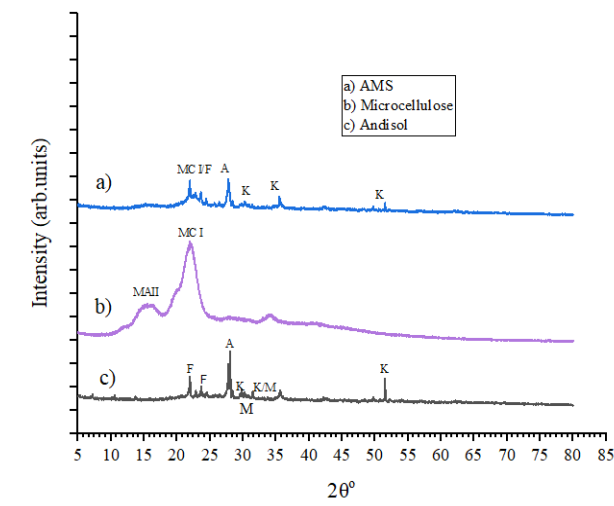


Figure 2. XRD graph of (a) AMS (b) microcrystalline cellulose, and (c) andisol

Andisol and microcrystalline cellulose are expected to be able to intercalate, where intercalation is the insertion of compounds in the interlayer space of a solid while maintaining its layered structure. This method will enlarge the pores of the material because the intercalation (inserted compound) will shift the layers or open between layers to expand [23]. Intercalation will affect the hydrogen bonding of the adsorbent. Cellulose is a material that is more likely to be deprotonated at the CH_2OH to CH_2O^- group than andisol. Andisol have van der waals bonds, so water can easily enter. Then, andisol will be protonated at OH group in silanol or aluminol to become OH_2^+ . Hence, CH_2O^- ion of cellulose binds to OH_2^+ ion of andisol [17]. However, andisol and microcrystalline cellulose cannot be composites, this can be seen from the FTIR and XRD data which is indicated by the absence of new peaks on the AMS adsorbent graph, which means that there is no chemical bond between the two materials. Figure 3 shows the SEM data of AMS in which long-shaped microcrystalline cellulose ($3.2 \mu\text{m}$) cannot be adsorbed into spherical andisols due to the smaller pore diameter of andisol, which is nanometers compared to the size of microcrystalline cellulose, which is micrometres [24]. This indicates that there is no physical interaction between andisol and microcrystalline cellulose.

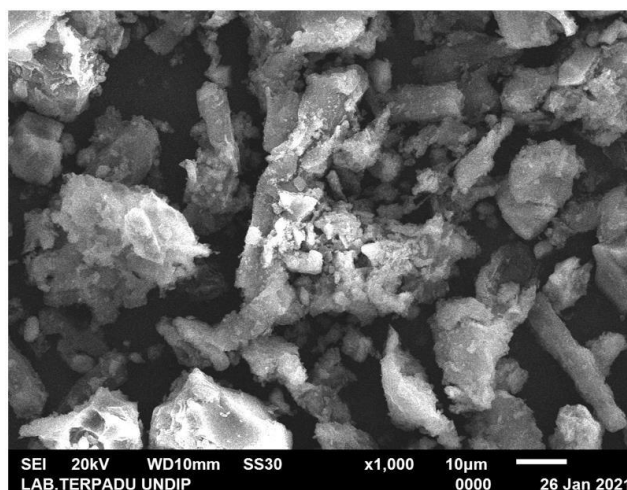


Figure 3. SEM data of AMS

Table 1 shows the data from the SAA andisol, microcrystalline cellulose, and AMS. The surface area of BET AMS was not higher than that of andisol and microcrystalline cellulose. The surface area of

AMS is smaller than the other two adsorbents due to its largest particle size. Therefore, the larger particle size causes a decrease in the adsorption ability [14]. A large surface area does not guarantee high reactivity, but the distribution of pore size also has an effect. Large pore volume and pore diameter also affect the increase in adsorption capacity [25]. Therefore, although the surface area of AMS is lower than that of andisol and microcrystalline cellulose because the volume and diameter of the pores have almost the same size, the adsorption capacity is also the same or there is no significant difference.

Table 1. SAA analysis of andisol, microcrystalline cellulose, and AMS

Material	S_{BET} (m^2/g)	V_{BET} (cc/g)	D_{BET} (nm)	S_{BJH} (m^2/g)	V_{BJH} (cc/g)	D_{BJH} (nm)
Andisol	25.92	0.093	14.40	29.23	0.094	3.82
Microcrystalline cellulose	26.60	0.034	5.14	15.72	0.027	3.77
AMS	18.60	0.056	11.96	21.00	0,058	3.78

3.2. Discussion AO adsorption by AMS

3.2.1. Variation of adsorbent ratio

Figure 4 describes the results of the adsorption process of various adsorbent ratios. All adsorbents used had a mass of 0.1 g for each comparison. AO solution is known to be at a concentration of 20 mg/L and a contact time of 30 minutes. The data from the adsorption process of AO on the variation of the adsorbent ratio did not have optimum results. All adsorbents have good efficiency and can adsorb more than 90% of AO. The use of AMS1 and AMS5 has no difference when used as AO adsorbents. The adsorbent that adsorbs the least AO is AMS4, then for the next variation, the adsorbent which absorbs the most AO is the ratio of AMS3 as much as 96.51% with an adsorption capacity of 3.86 mg/g. In this study, the adsorption capacity value by AMS can be said to have the same value as the adsorption capacity of andisol and microcrystalline cellulose. AMS does not have a high adsorption capacity because cellulose cannot enter the pores of the andisol so the active group of this adsorbent does not increase. So, the results cannot be almost the same, then the adsorption capacity is also the same value or there is no significant difference, it increases significantly.

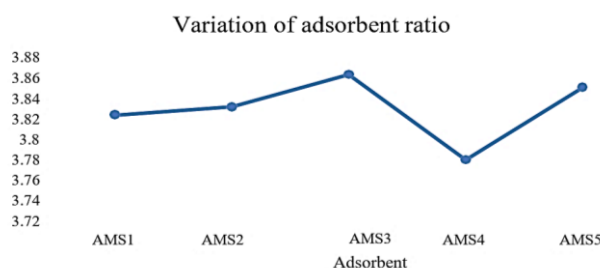


Figure 4. AO adsorption at the different adsorbent ratio

3.2.2. Variations of pH

The adsorption conditions at various pH were 0.1 gram (mass ratio of AMS adsorbent 1:1), 20 mg/L AO, and 30 minutes for contact time. Figure 5 is a graph of AO adsorption results at different pH conditions. The optimum condition occurs at pH 7, which is as much as 99.22% (4.15 mg/g) AO is adsorbed. This is because the H^+ and OH^- ions are equal so there is no competition between AO and H^+ ions. At pH 5, 31.48% (1.10 mg/g) AO was adsorbed, which was the least compared to other pH conditions, where highly acidic adsorption conditions would cause competition between hydrogen ions and AO when bound to AMS. AO is adsorbed up to 98.38% (5.01 mg/g) at pH 6, but to facilitate this research, pH 7 will be used as the pH condition in the next variation. Alkaline conditions, namely pH 8 AO which was adsorbed down, but still more than 50% (1.44 mg/g). At alkaline pH, OH^- ions will be slightly more than at pH 7, therefore, OH^- ions will also bind to AO. Then, when filtering was carried out, the AO which was bound to the OH^- ion was still soluble in the solution or was not entangled on the filter paper because it did not bind to AMS [1]. Figure 6 describes the adsorption reaction of AO by AMS.

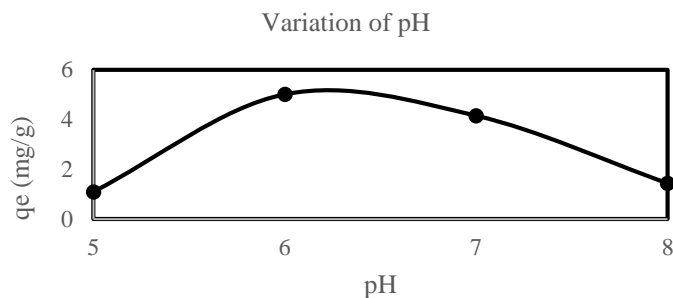


Figure 5. AO adsorption at different pH variations

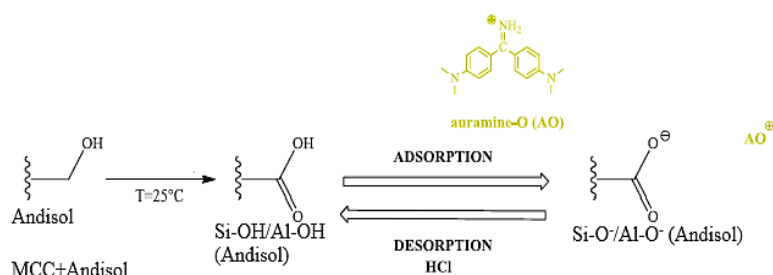


Figure 6. AMS reaction during the AO adsorption process [1]

3.2.3. Variations of contact time

Figure 7 shows the results of the variation in contact time of AMS with AO. The adsorption process at various contact times has a pH of 7, an adsorbent mass of 0.1 grams, 20 mg/L AO, and a contact time of 5-120 minutes. The time required for adsorption does not take a long time, namely 5 minutes, which reaches an efficiency of 92.73% (3.88 mg/g). Thus, the variation of concentration using a contact time of 5 minutes. The adsorption process with a contact time of up to 2 hours still has a good efficiency of 90%. The contact time that most adsorbed AO was 30 minutes, which was 98.2% (4.08 mg/g). During the first 5 minutes, the active sites of AMS were still unfilled and the availability of dye ions was still high, therefore the adsorption increased rapidly. Then, the longer the contact time, the active site has been filled and unbound dye ions will remain [13].

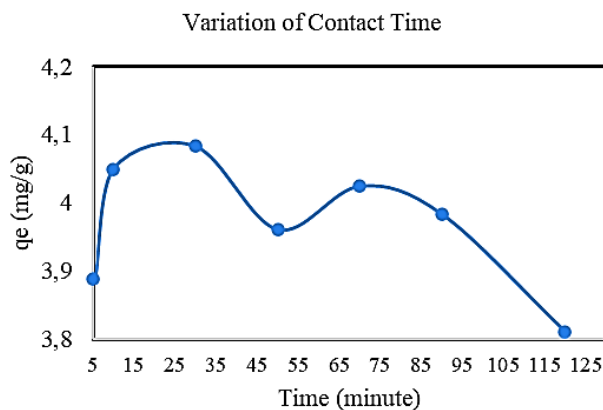


Figure 7. AO adsorption at different contact time variations

3.2.4. Variations of concentration

Figure 8 shows the results of the adsorption of AO at pH 7, a contact time of 5 minutes, and a solution volume of 20 ml. Each AO at a concentration of 20, 40, 60, 80, and 100 mg/L. At 20 mg/L AO concentration, the efficiency obtained was 93.4% (3.90 mg/g). The maximum concentration that can be adsorbed is at a concentration of 40 mg/L, which is 98.745% (8.05 mg/g). As the concentration increases, the adsorption strength of the AMS adsorbent will decrease, due to the excess of AO molecules that cannot be adsorbed, in which the number of active sites is limited and has been filled [13]. The concentration of 100 mg/L has the lowest efficiency value of 24.662% (6.81 mg/g).

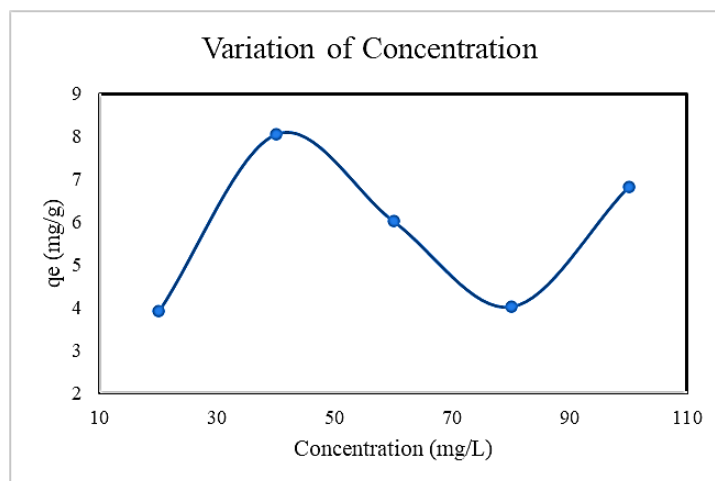


Figure 8. AO adsorption at different concentrations

3.2.5. Adsorption kinetics

Adsorption kinetics is used to determine the effect of contact time and the mechanism that occurs in the adsorption process. The adsorption kinetics can be determined by pairing the results obtained with first-order, second-order, pseudo-first-order, and pseudo-second-order equations. From the following Figure 7 and Table 2, it can be seen that a straight graph has been produced. It can be inferred from the adsorption kinetics data that the adsorption process follows the pseudo-second order model. This means that the adsorption process that occurs is dependent on the adsorption ability of each solid phase. It can be explained that the adsorption capacity obtained is directly proportional to the active site owned by the adsorbent used [26]. The pseudo-second-order model also explains that each AO ion is adsorbed by both adsorption sites which allows for a binuclear bond to occur [27]. The adsorption time required to reach equilibrium in the first-order model is faster than in the second-order pseudo model. The adsorption capacity value of the pseudo second order model is 4.0 mg/g.

Table 2. Adsorption kinetics equations

Adsorption Kinetics	Equation	Explanation
First order	$\ln C_e = \ln C_0 - kt$	C_e = concentration at t C_0 = concentration at t = 0
Second order	$\frac{1}{C_e} - \frac{1}{C_0} = kt$	k = kinetic constant (minute ⁻¹) t = time (minute) [29].
Pseudo-first-order	$(q_e - qt) = \ln q_e - (k_1 t)$	q_e and qt = the amount of adsorbate adsorbed at equilibrium and a certain time,
Pseudo-second-order	$\frac{t}{qt} = \frac{1}{k_2 q_e^2} + \frac{t}{q_e}$	k_1 = adsorption rate constant (minute) k_2 the unit is g/mg/min [26].

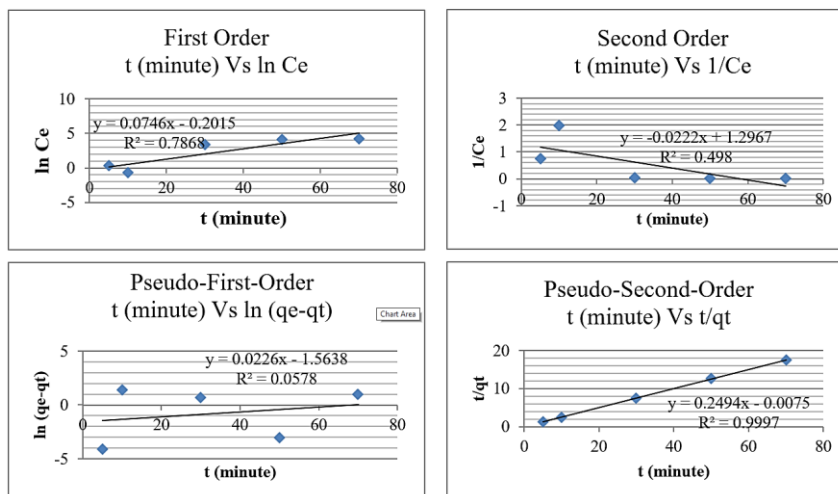


Figure 7. First order, second order, pseudo-first-order, and pseudo-second order adsorption kinetics model

3.2.6. Adsorption isotherm

The adsorption isotherm can explain the relationship between the adsorbate concentration and the adsorbate concentration remaining in the liquid at equilibrium time [28]. The adsorption isotherm can be determined by using the results of the adsorption process of AO by AMS at various concentrations. Experimental data are included in the Langmuir and Freundlich equations which are shown in Table 3.

Table 3. Adsorption isotherm equations

Adsorption Isotherm	Equation	Explanation
Langmuir	$\frac{1}{q_e} = \frac{1}{Q} + \left(\frac{1}{Qb}\right) \frac{1}{C_e}$	q_e = equilibrium adsorption capacity (mg/g) Q = maximum amount of adsorption to form an entire monolayer on the adsorbent surface(mg/g) C_e = adsorbate concentration (mg/L)
Freundlich	$\ln q_e = \ln K_f + \frac{1}{n} \ln C_e$	b = Langmuir's constant relating to binding site affinity K_F and n = Freundlich parameter [29], [30]

The adsorption isotherm used in this study is the Langmuir and Freundlich isotherm. The adsorption isotherm can be seen in Figure 8 that the adsorption isotherm model follows the Langmuir model, where the R^2 value is 0.8678 (adsorption capacity = 5.23 mg/g), while the Freundlich isotherm model has an R^2 value = 0.0295 (adsorption capacity = 5.83 mg/g). However, the adsorption capacity of the Freundlich model is higher than that of the Langmuir model. The AO adsorption process by AMS tends to follow the Langmuir isotherm model. This shows that the adsorption process of AO on the AMS takes place chemically and the absorption mechanism is a monolayer on the surface of the adsorbent [30], [31]. The active sites on the surface of microcellulose, namely OH and Si-O or Al-O from andisol are the most important in this adsorption process.

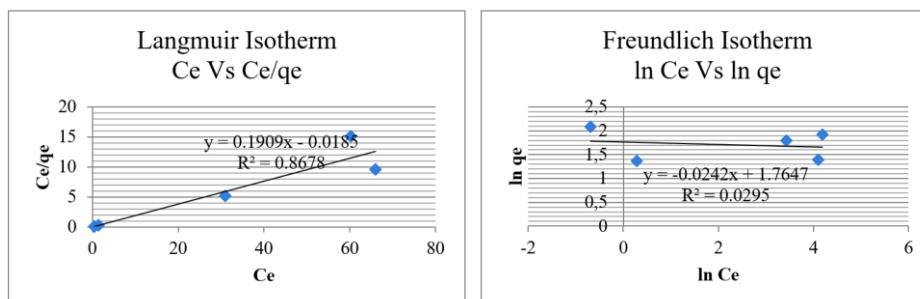


Figure 8. Langmuir and Freundlich adsorption isotherm model

4. CONCLUSION

The conclusion of this research is that the surface area of BET andisol is 25.92 m²/g while microcrystalline cellulose has a surface area of BET 26.60 m²/g. Then, the AMS adsorbent has a BET surface area of 18.60 m²/g with a pore diameter of 14.40 nm. The maximum yield of AO adsorption by AMS3 was at pH 7, the optimum contact time was 5 minutes, the maximum concentration was 40 mg/L, and the maximum adsorbent ratio was AMS3 (andisol-microcrystalline cellulose 1:1). The adsorption capacity of AMS3 to AO was 5.24 mg/g. Although andisol and microcrystalline cellulose cannot be composites, this study can explain that andisol or microcrystalline cellulose is a good adsorbent for AO.

REFERENCES

- [1] L. R. Martins, J. A. V. Rodrigues, O. F. H. Adarme, T. M. S. Melo, L. V. A. Gurgel, and L. F. Gil, "Optimization of cellulose and sugarcane bagasse oxidation: Application for adsorptive removal of crystal violet and auramine-O from aqueous solution," *Journal of Colloid and Interface Science*, vol. 494, pp. 223–241, May 2017, doi: 10.1016/j.jcis.2017.01.085.
- [2] T. Mahmud, "Biosorption of Auramine O and Drimarene dyes from aqueous solutions using seed powder of *Diospyros lotus*," *International Journal of Environment and Sustainability*, vol. 6, no. 3, Dec. 2018, doi: 10.24102/ijes.v6i3.895.
- [3] S. Shi, M. Zhang, C. Ling, W. Hou, and Z. Yan, "Extraction and characterization of microcrystalline cellulose from waste cotton fabrics via hydrothermal method," *Waste Management*, vol. 82, pp. 139–146, Dec. 2018, doi: 10.1016/j.wasman.2018.10.023.
- [4] C. Qi *et al.*, "Adsorption Kinetics and Thermodynamics of Auramine-O on Sugarcane Leaf-Based Activated Carbon," *Journal of Dispersion Science and Technology*, vol. 36, no. 9, pp. 1257–1263, Sep. 2015, doi: 10.1080/01932691.2014.973036.
- [5] S. N. Islamiyah and T. Koestiari, "Use of granular activated carbon as an adsorbent for Cu (II) metal in Kenjeran seawater, (Penggunaan Karbon Aktif Granular Sebagai Adsorben Logam Cu (II) Di Air Laut Kenjeran)," *UNESA Journal of Chemistry*, vol. 3, no. 3, pp. 164–169, 2018, doi: 10.26740/ujc.v3n3.p%25p.
- [6] M. Nanzyo, S. Shoji, and R. Dahlgren, "Chapter 7 Physical Characteristics of Volcanic Ash Soils," 1993, pp. 189–207. doi: 10.1016/S0166-2481(08)70268-X.
- [7] V. Neall, "Volcanic Soils," *Land Use, Land Cover And Soil Sciences*, vol. vii, 2000, [Online]. Available: https://www.researchgate.net/publication/238789918_Volcanic_soils
- [8] P. Pranoto, "Fabrication of Sugar Palm Fiber/Andisol Soil Composites for Iron(III) ion Removal in Aqueous Solution," *Oriental Journal of Chemistry*, vol. 34, no. 1, pp. 346–351, Feb. 2018, doi: 10.13005/ojc/340137.
- [9] J. George and S. S N, "Cellulose nanocrystals: synthesis, functional properties, and applications," *Nanotechnology, Science and Applications*, vol. 8, pp. 45–54, Nov. 2015, doi: 10.2147/NSA.S64386.
- [10] P. Tyagi *et al.*, "High-Strength Antibacterial Chitosan–Cellulose Nanocrystal Composite Tissue Paper," *Langmuir*, vol. 35, no. 1, pp. 104–112, Jan. 2019, doi: 10.1021/acs.langmuir.8b02655.
- [11] M. E. El-Naggar *et al.*, "Synthesis, characterization and adsorption properties of microcrystalline cellulose based nanogel for dyes and heavy metals removal," *International Journal of Biological Macromolecules*, vol. 113, pp. 248–258, Jul. 2018, doi: 10.1016/j.ijbiomac.2018.02.126.
- [12] A. A. B. Haryanto, A. H. Ramelan, M. T. H. Sri Budiastuti, and Pranoto, "Preparation and characterization of andisol-zeolite-fly ash-activated carbon (AZFC) as potential adsorbent for metal ion removal," in *AIP Conference Proceedings*, 2020, vol. 2296, p. 2296. doi: 10.1063/5.0032586.
- [13] K. B. Tan, A. Z. Abdullah, B. A. Horri, and B. Salamatinia, "Adsorption mechanism of microcrystalline cellulose as green adsorbent for the removal of Cationic methylene blue dye," *Journal of the Chemical Society of Pakistan*, vol. 38, no. 4, pp. 651–664, 2016.
- [14] S. Karimi, M. Tavakkoli Yaraki, and R. R. Karri, "A comprehensive review of the adsorption mechanisms and factors influencing the adsorption process from the perspective of bioethanol dehydration," *Renewable and Sustainable Energy Reviews*, vol. 107, pp. 535–553, Jun. 2019, doi: 10.1016/j.rser.2019.03.025.
- [15] P. Pranoto, R. Rosariastuti, and A. Prihandoko, "Short Communication: The utilization and effectiveness test of andisol soil-bioball-Agrobacterium sp. toward heavy metal chrome removal," *Biodiversitas Journal of Biological Diversity*, vol. 19, no. 5, pp. 1955–1959, Sep. 2018, doi: 10.13057/biodiv/d190547.
- [16] P. Pranoto, C. Purnawan, and T. Utami, "Application of bekonang clay and andisol soil composites as copper (II) metal ion adsorbent in metal crafts wastewater," *Rasayan Journal of Chemistry*, vol. 11, no. 1, pp. 23–31, 2018, doi: 10.7324/RJC.2018.1111939.
- [17] S. P. Santoso *et al.*, "Preparation of nanocrystalline cellulose-montmorillonite composite via thermal radiation for liquid-phase adsorption," *Journal of Molecular Liquids*, vol. 233, pp. 29–37, May 2017, doi: 10.1016/j.molliq.2017.02.091.
- [18] S. O. Ginting and R. Mohadi, "Adsorption of congo red using kaolinite-cellulose adsorbent," *Science and Technology Indonesia*, vol. 2, no. 2, pp. 29–36, Jun. 2017, doi: 10.26554/sti.2017.2.2.29-36.
- [19] A. Kausar, R. Shahzad, J. Iqbal, N. Muhammad, S. M. Ibrahim, and M. Iqbal, "Development of new organic-inorganic, hybrid bionanocomposite from cellulose and clay for enhanced removal of Drimarine Yellow HF-3GL dye," *International Journal of Biological Macromolecules*, vol. 149, pp. 1059–1071, Apr. 2020, doi: 10.1016/j.ijbiomac.2020.02.012.
- [20] R. M. Sheltami, I. Abdullah, I. Ahmad, A. Dufresne, and H. Kargarzadeh, "Extraction of cellulose nanocrystals

- from mengkuang leaves (*Pandanus tectorius*),” *Carbohydrate Polymers*, vol. 88, no. 2, pp. 772–779, Apr. 2012, doi: 10.1016/j.carbpol.2012.01.062.
- [21] X. Kang, S. Kuga, C. Wang, Y. Zhao, M. Wu, and Y. Huang, “Green Preparation of Cellulose Nanocrystal and Its Application,” *ACS Sustainable Chemistry & Engineering*, vol. 6, no. 3, pp. 2954–2960, Mar. 2018, doi: 10.1021/acssuschemeng.7b02363.
- [22] W. T. Wulandari, A. Rochliadi, and I. M. Arcana, “Nanocellulose prepared by acid hydrolysis of isolated cellulose from sugarcane bagasse,” *IOP Conference Series: Materials Science and Engineering*, vol. 107, p. 012045, Feb. 2016, doi: 10.1088/1757-899X/107/1/012045.
- [23] Fitriyah, “Intercalation of xylene orange in Lampung natural zeolite as a modified zeolite electrode, (Intercalasi Xilenol Orange Pada Zeolit Alam Lampung sebagai Elektroda Zeolit Termodifikasi),” *Jurnal Kimia dan Pendidikan*, vol. 1, no. 2, pp. 162–175, 2016, doi: 10.30870/educhemia.v1i2.770.
- [24] W. Astuti, I. M. Bendiyasa, E. T. Wahyuni, and A. Prasetya, “The Effect of Coal Fly Ash Crystallinity toward Methyl Violet Adsorption Capacity,” *ASEAN Journal of Chemical Engineering*, vol. 10, no. 1, pp. 8–14, 2010, doi: 10.22146/ajche.50090.
- [25] A. S. González-Ugarte, I. Hafez, and M. Tajvidi, “Characterization and properties of hybrid foams from nanocellulose and kaolin-microfibrillated cellulose composite,” *Scientific Reports*, vol. 10, no. 1, p. 17459, Oct. 2020, doi: 10.1038/s41598-020-73899-z.
- [26] U. A. Edet and A. O. Ifelebuegu, “Kinetics, Isotherms, and Thermodynamic Modeling of the Adsorption of Phosphates from Model Wastewater Using Recycled Brick Waste,” *Processes*, vol. 8, no. 6, p. 665, Jun. 2020, doi: 10.3390/pr8060665.
- [27] M. Nilsson, A. Mhryyan, S. Valizadeh, and M. Strømme, “Mesopore Structure of Microcrystalline Cellulose Tablets Characterized by Nitrogen Adsorption and SEM: The Influence on Water-Induced Ionic Conduction,” *The Journal of Physical Chemistry B*, vol. 110, no. 32, pp. 15776–15781, Aug. 2006, doi: 10.1021/jp055858v.
- [28] A. S. Sanjaya and R. P. Agustine, “Study Of Pb Adsorption Kinetics Using Active Charcoal From Banana Peels, (Studi Kinetika Adsorpsi Pb Menggunakan Arang Aktif Dari Kulit Pisang),” *Konversi*, vol. 4, no. 1, p. 17, Apr. 2015, doi: 10.20527/k.v4i1.261.
- [29] Saruchi and V. Kumar, “Adsorption kinetics and isotherms for the removal of rhodamine B dye and Pb²⁺ ions from aqueous solutions by a hybrid ion-exchanger,” *Arabian Journal of Chemistry*, vol. 12, no. 3, pp. 316–329, Mar. 2019, doi: 10.1016/j.arabjc.2016.11.009.
- [30] P. Liu, “Adsorption Behavior of Heavy Metal Ions From Aqueous Medium on Nanocellulose,” Luleå University of Technology, 2015. [Online]. Available: <https://www.diva-portal.org/smash/get/diva2:999523/FULLTEXT01.pdf>.
- [31] M. Goswami and A. M. Das, “Synthesis and characterization of a biodegradable Cellulose acetate-montmorillonite composite for effective adsorption of Eosin Y,” *Carbohydrate Polymers*, vol. 206, pp. 863–872, Feb. 2019, doi: 10.1016/j.carbpol.2018.11.040.